

1     **Geometrical analysis of bi-stretch auxetic woven fabric based on re-entrant**  
2    **hexagonal geometry**

3    Adeel Zulifqar and Hong Hu\*

4  
5            Institute of Textiles and Clothing, The Hong Kong Polytechnic University, Hung Hom, Hong Kong

6    \*The corresponding author: [hu.hong@polyu.edu.hk](mailto:hu.hong@polyu.edu.hk)  
7

8     **Abstract**

9     This paper reports a study on the geometrical analysis of bi-stretch auxetic woven fabric based on  
10    a re-entrant hexagonal geometry. The fabrics was first designed and fabricated. Then, the fabric  
11    was subjected to tensile tests and changes in the geometry of the fabric structural unit cell at  
12    different tensile strains were observed when stretched either in warp or weft direction. Based on  
13    the observations, a geometrical model was proposed for each stretch direction and used to establish  
14    the relationship between Poisson's ratio and tensile strain. The semi-empirical equations for both  
15    stretch directions were finally obtained by fitting geometrical parameters with experimental  
16    results. It is expected that the semi-empirical equations obtained in this study could be used in the  
17    design and prediction of the auxetic behaviour of bi-stretch auxetic woven fabrics made with the  
18    same type of materials and geometry, but with different values of geometrical parameters.

19    **Keywords:** auxetic woven fabrics, negative Poisson's ratio, deformation behaviour, geometrical  
20    analysis

21    **1. Introduction**

22    Auxetic materials have negative Poisson's ratio (NPR) [1-3]. Unlike conventional materials,  
23    auxetics laterally expand when stretched or laterally contract when compressed. To date, auxetic  
24    textile materials including auxetic polymers, fibers, yarns, semi-auxetic yarns and fabrics have  
25    been developed and investigated [4-6]. Among the auxetic textile materials, the auxetic fabrics  
26    have come to the forefront in modern times and have been gaining more and more interest of the  
27    textile scientists. Auxetic fabrics are superior to conventional fabrics because of their unusual

1 properties, such as synclastic behaviour for better formability [7], improved comfort, form fitting  
2 at joint parts [8] and increased porosity under stress [9-11]. The most straightforward approach of  
3 producing the auxetic fabrics is to directly use auxetic yarns either in warp or weft direction and  
4 weaving technology. Following this approach, two types of auxetic woven fabrics were made using  
5 helix auxetic yarns (HAYs) in the weft. The first type was auxetic woven fabrics produced with  
6 plain, twill and satin weaves. Among the three fabrics, the plain and twill fabrics exhibited most  
7 auxeticity and the satin woven fabric was found less auxetic [9]. The second type was a plain-  
8 woven fabric which exhibited an in-plane NPR up to -0.1, only when the fabric was tested under  
9 thickness restrictions by glass plates [10]. Besides these fabrics, a 2-ply plain narrow woven fabric  
10 was also produced by using HAYs as warp yarns. This fabric showed an in-plane NPR of -0.1 at  
11 32% of tensile strain and increased porosity at 80N of applied tension [12]. Recently, plied auxetic  
12 yarns were used to fabricate woven fabrics and it was found that the alternative arrangement of S-  
13 and Z-twisted plied auxetic yarns in a woven fabric could produce a higher NPR. It was also  
14 reported that the NPR effect of HAYs could not be fully utilized in woven fabrics due to constraints  
15 of woven fabric structure [13].

16 The other approach of producing auxetic fabrics involves using non-auxetic yarns and knitting or  
17 weaving technology to produce auxetic fabrics. Because the auxetic behaviour is linked with the  
18 geometrical arrangements of the structural units, therefore this approach is based on the technique  
19 of realizing auxetic geometries into fabric structures [5]. The knitted fabrics produced by adopting  
20 this approach include auxetic warp knitted fabrics made from rotational hexagonal loops geometry  
21 [14], double arrowhead geometry[15], re-entrant hexagonal (REH) geometry [16-18] and spacer  
22 structure [19], and auxetic weft knitted fabrics produced with foldable geometries [20-22], rotating  
23 rectangle geometry [21], REH geometry, double arrowhead geometry [23] and tubular fabrics[24].  
24 However, these auxetic fabrics still have certain limitations. Low structural stability, higher  
25 thickness, low modulus and low strength are some of drawbacks of these fabrics which restrict  
26 their applications in garments and other areas. Adopting the same approach, uni-stretch auxetic  
27 woven fabrics were also produced based on foldable geometries, rotating rectangle geometry and  
28 REH geometry [2] through the creation of the phenomenon of differential shrinkage or non-  
29 uniform contraction profile within the fabric structural unit cell by using elastic and non-elastic  
30 yarns together with loose and tight weaves. However, these fabrics also have some major  
31 drawbacks such as extensibility and smaller auxetic effect only in one direction. Most recently, it  
32 was reported that developing bi-stretch auxetic woven fabric having extensibility and larger

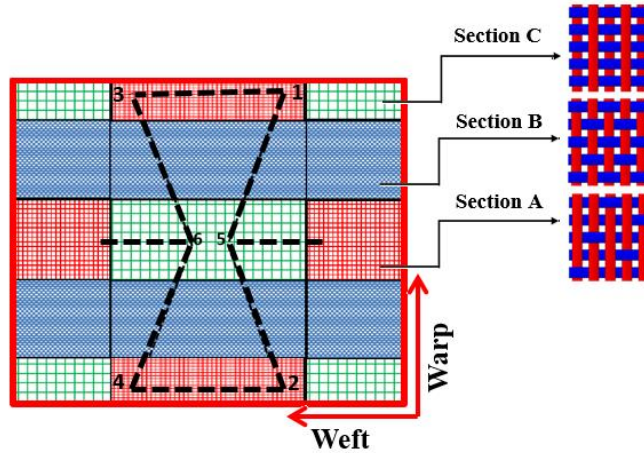
1 auxetic effect in both directions is possible by using the same technique as used in development  
2 of uni-stretch auxetic woven fabrics. The first reported fabrics were produced based on the foldable  
3 geometry with NPR up to -0.36 and -0.27 when stretched along the warp and weft direction,  
4 respectively [25]. Besides this, the development of a new bi-stretch auxetic woven fabrics based  
5 on an approximation of REH geometry was also reported [26]. The study has shown that the  
6 developed bi-stretch woven fabrics have NPR effect in both principal directions. These fabrics  
7 may have a great potential for clothing application, such as highly stretchable sport garment like a  
8 riding kit for bikers which can cast itself to different body shapes [27], stretchable textile carriers  
9 [28] and denim products providing comfort and ability to mold and move easily in accordance  
10 with body movements [29], etc. Although the reported studies can provide a systematic  
11 information on the design and fabrication of these fabrics, the relationships between the  
12 geometrical parameters and tensile deformation are still not explored. In this paper, a geometrical  
13 analysis of such fabrics is conducted to establish these relationships, since they are very helpful in  
14 design and prediction of auxetic effect of fabrics for specific applications. The fabric based on  
15 REH geometry was chosen for this analysis because it has already been reported as a potential  
16 candidate among auxetic geometries which can easily be realized into woven fabric structure [2].  
17 In addition, because the unit cell of REH geometry is simple, the geometrical analysis can be  
18 carried out more straightforwardly. In order to facilitate the geometrical analysis, the fabric was  
19 first tested under a uniaxial extension to observe the changes in the geometry of its structural unit  
20 cell at different tensile strains. Then, based on the observations, a geometrical model was proposed  
21 for each stretch direction. From the geometrical analysis, the semi-empirical equations between  
22 the Poisson's ratio and tensile strain were finally established for both weft and warp stretch  
23 directions. The study shows that the established semi-empirical equations fit well with  
24 experimental results. Therefore, they could be used in the design and prediction of bi-stretch  
25 auxetic woven fabrics with different values of geometrical parameters.

## 26 **2. Experimental**

### 27 **2.1 Design and fabrication of auxetic woven fabrics**

28 Before conducting the geometrical analysis, bi-stretch auxetic woven fabrics based on REH  
29 geometry were first designed and fabricated. A special interlacement pattern having loose and tight  
30 weaves at different sections of the unit cell as reported by the authors [26] and shown in Figure 1  
31 was used to achieve the geometrical configurations of the hexagonal unit cells into the fabric

1 structure. It can be seen that the unit cell of the interlacement pattern includes three sections A, B  
 2 and C, which are formed with different weaving tightness. While the sections A at ribs 1-3 and 2-  
 3 4 are woven with loose (4/1) weave, the sections B next to the ribs 1-3 and 2-4 are woven with  
 4 tight (1/1) weave. The central section C is also woven with loose weave in such a way that the  
 5 warp yarns are free of interlacement and raise above the weft yarns alternately. Thus, the order of  
 6 weaving tightness of three sections is  $B > A > C$ .

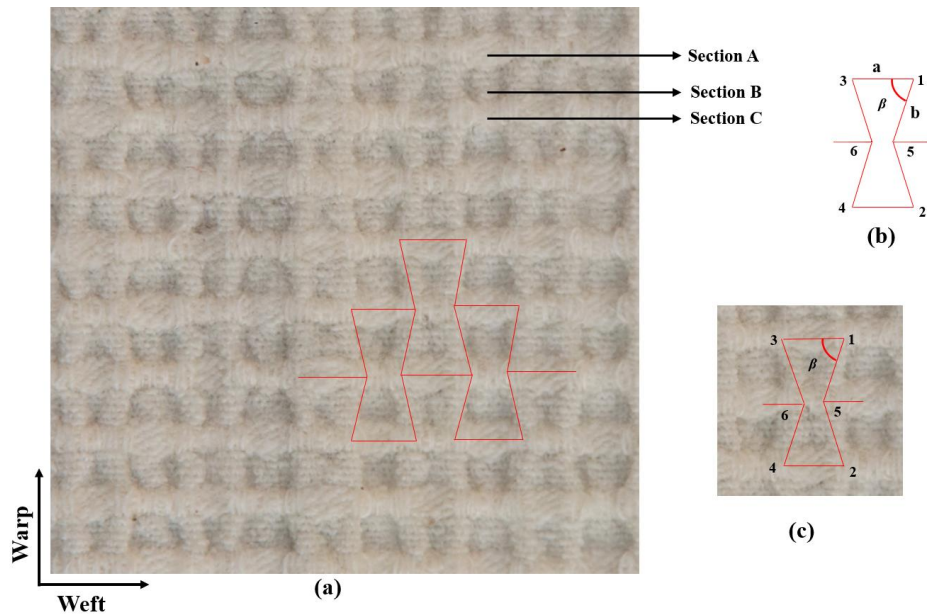


7

8 **Figure 1. Schematic illustration of loose and tight weaves placement in the unit cell of designed interlacement pattern**

9 One of the fabrics produced based on this interlacement pattern is shown in Figure 2(a), in which  
 10 the three different sections of the unit cell, namely A, B and C are clearly indicated. A unit cell of  
 11 the fabric geometry is shown in Figure 2(b), in which segments 1-3 and 2-4 are the horizontal ribs  
 12 named as  $a$ , whereas segments 1-5, 5-2, 3-6 and 6-4 are the diagonal ribs named as  $b$ . The basic  
 13 unit cell of the fabric structure with outline of hexagonal unit cell is shown in Figure 2(c). When  
 14 this structure is stretched in either direction, the diagonal rib segments  $b$  will move to the  
 15 horizontal disposition, leading to an increase of the distance between point 5 and 6. As a result,  
 16 the dimensions of the whole structure increase and the auxetic effect is achieved. It can be seen  
 17 that the geometrical parameters  $a$ ,  $b$  and angle  $\beta$  formed between  $a$  and  $b$  determine the  
 18 geometrical features of the structure at the initial state. In order to get the semi-empirical equations  
 19 and verification of the semi-empirical equations, two fabrics namely Fabric-A and Fabric-B with  
 20 different values of  $\beta$  were designed and fabricated on a rapier weaving machine (Model: SL8900S)  
 21 manufactured by CCI Intech (Taiwan), equipped with the option of using two warp beams having  
 22 separate controls of warp yarn let off motion and warp yarn tension for both beams. 14.8 Tex core

1 spun cotton spandex yarn was used as elastic yarn and 14.8 Tex cotton spun yarn was used as non-  
 2 elastic yarn. The core of the elastic yarn was a 4.44 Tex spandex filament. The weft and warp  
 3 thread densities used were 31.50/cm and 25.20/cm, respectively. In addition, Polyvinyl Alcohol  
 4 (PVA) having specifications as PH: 5-7, Hydrolysis: 86.5-89, Viscosity: 20.5 to 24.5 CP's and Ash  
 5 contents: 0.7% was applied on the surface of warp yarns as a sizing material.



6

7 **Figure 2. A bi-stretch auxetic woven fabric based on REH geometry: (a) fabric face showing geometrical configuration;**  
 8 **(b) hexagonal unit cell; (c) basic unit of fabric structure with outline of hexagonal unit cell.**

9 For both fabrics, alternate elastic and non-elastic yarns were used in warp direction. However, yarn  
 10 arrangements in weft direction were different. In case of Fabric-A, alternate elastic and non-elastic  
 11 yarns were used at section A and B, while only elastic yarn was used at central section C. In Fabric-  
 12 B, only elastic yarn was used at all three sections. It is important to mention that because of using  
 13 only elastic yarns in weft for Fabric-B, the weft yarns may retract if the selvedge grip is not strong  
 14 enough. To avoid this problem, separate heald frames for selvedge were used. To eliminate sizing  
 15 material, the two fabrics after weaving were subjected to a washing process with lukewarm water  
 16 (40-45°C) for 45 minutes, followed by a drying and relaxation at room temperature for 24 hours.  
 17 Therefore, after the treatment the fabrics with different  $\beta$  were obtained. To determine the  
 18 geometrical parameters of both fabrics, the outlines of the unit cell were marked on the original  
 19 fabric photos, and the values of  $a$ ,  $b$  and  $\beta$  were measured using a screen ruler and screen

1 protector. Then, the real lengths of  $a$  and  $b$  were obtained by relative scale. The obtained mean  
 2 values of geometrical parameters for both fabrics are listed in Table 1.

3

4 **Table 1. Geometrical parameters of bi-stretch auxetic woven fabrics based on REH geometry**  
 5

Fabric ID	a (mm)	b (mm)	$\beta$ (Degree)
Fabric-A	4.15	2.69	55.63
Fabric-B	4.15	2.69	56.98

## 6 2.2 Tensile tests

7 The tensile tests were carried out in both weft and warp directions on an Instron 5566 tensile testing  
 8 machine. The capacity of the load cell used was 10kN. The gauge length and tensile speed were set  
 9 at 150mm and 30mm/min, respectively and jaws of size 76.2mm x 25.4mm were used. The testing  
 10 setup is shown in Figure 3. A set of three fabric strips of dimension 50mm×200mm were cut for  
 11 each sample with the length in the warp and in weft, respectively. The central point of the fabric  
 12 strip was first located and then four points were marked with the central point at 20mm to facilitate  
 13 recording the information of fabric deformation during the tensile test. The tensile test was video  
 14 recorded by using a camera (Canon EOS 800D). The video resolution used was Full HD (1920 x  
 15 1080). The photographs were then extracted with a time interval of 15s or after each 5% extension.  
 16 The distances of the marks in the photographs were measured via a screen ruler for both the free  
 17 state and stretched state with an accuracy of 4.66 px/mm. The engineering strains of the fabric  
 18 structure in both tensile direction and transversal direction were then calculated based on the  
 19 measured distances by using equations 1 and 2, respectively.

$$20 \quad \varepsilon_a = \frac{x - x_0}{x_0} \quad (1)$$

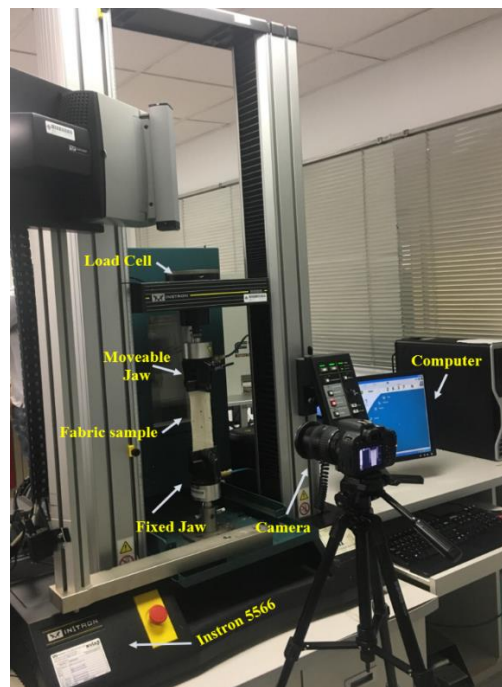
$$21 \quad \varepsilon_t = \frac{y - y_0}{y_0} \quad (2)$$

22 Where  $\varepsilon_a$  is the tensile strain,  $x_0$  and  $x$  are the initial and deformed length in the tensile direction  
 23 respectively,  $\varepsilon_t$  is the transversal strain,  $y_0$  and  $y$  are the initial and deformed length in the

1 transversal direction respectively. Finally, the Poisson's ratio (PR)  $\nu$  was calculated using  
2 equation 3 [30]. The process was repeated for all three strips.

3 
$$\nu = -\frac{\epsilon_t}{\epsilon_a} \quad (3)$$

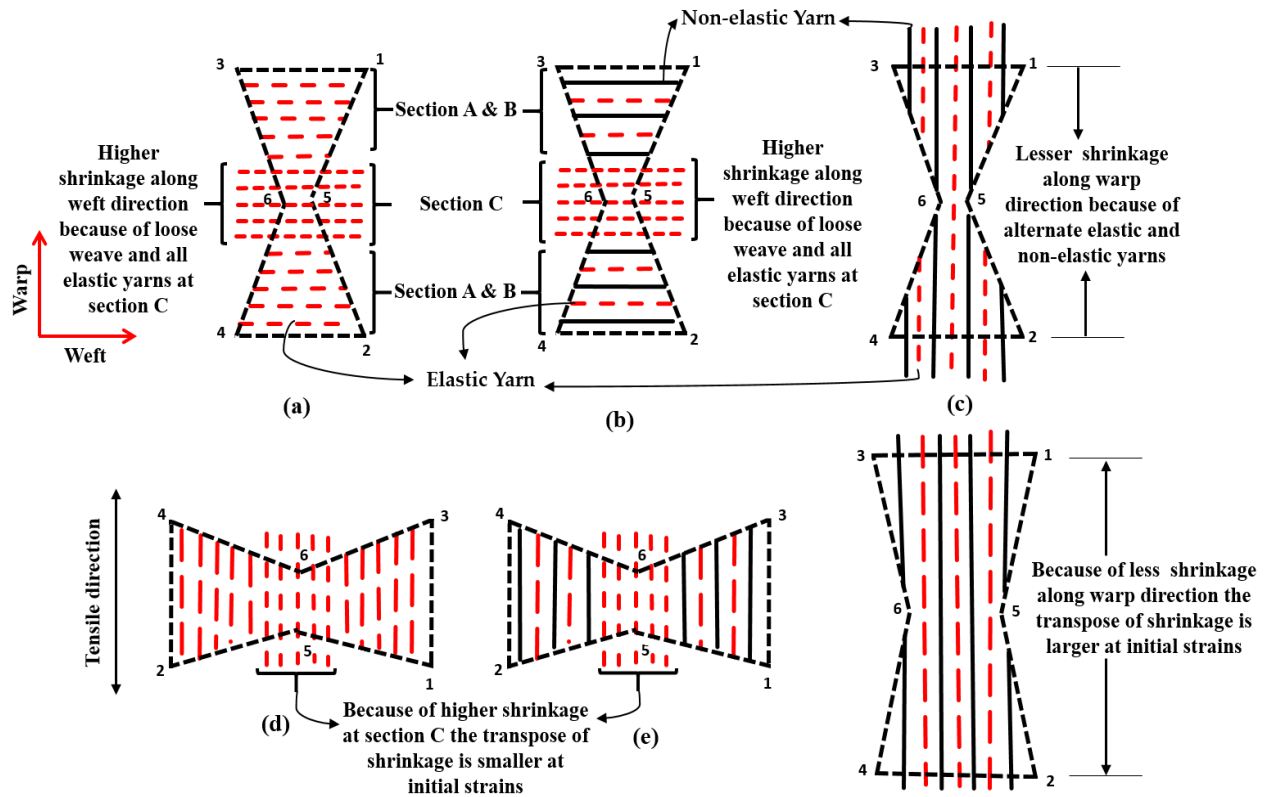
4 The PR was calculated at every 5% of tensile strain. This time of measurement was chosen to  
5 observe any change in dimensions even within 5% of tensile strain. The PR versus tensile strain  
6 curve was generated by using the data of the tensile test.



7  
8 **Figure 3.** Testing setup for the tensile test of the auxetic woven fabric.

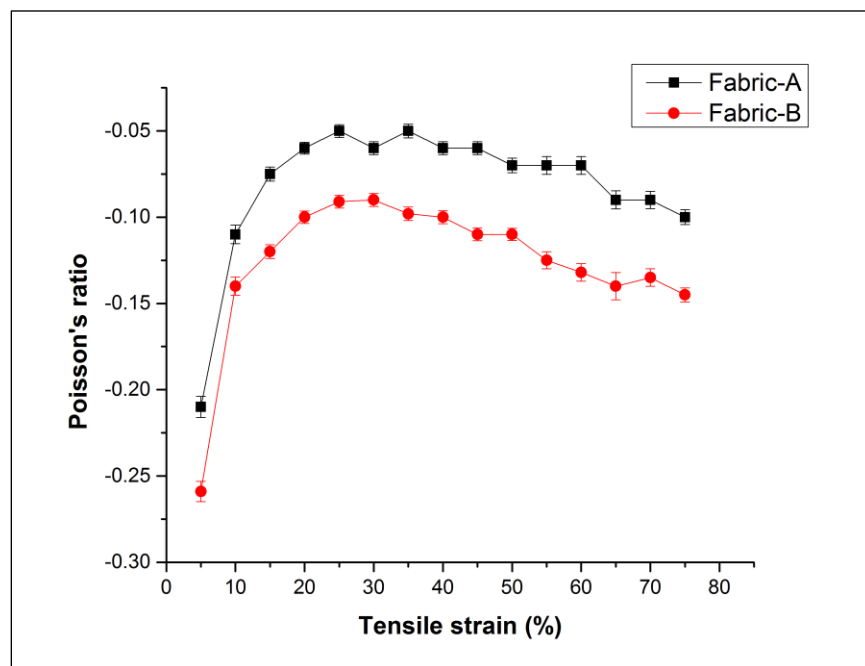
9 Upon stretching along warp or weft direction, the fabric undergoes tensile deformation and the  
10 shrinkage is transposed. This makes the distance between point 5 and 6 to increase and the fabric  
11 expands in the transverse direction producing the auxetic effect. The PR versus tensile strain curves  
12 of the two fabrics, when stretched in two principal directions, are shown in Figure 5 and Figure 6,  
13 respectively. It can be seen that the auxetic effect is produced in both warp and weft directions.  
14 However, the auxetic effect when stretched in the warp direction is higher than that when stretched  
15 in the weft direction. It can also be seen that the auxetic effect of the fabric rapidly decreases with  
16 the increase of tensile strain at the initial stage of stretch and reaches its lowest level when the  
17 strain reaches about 30%. Then, the auxetic effect almost keeps stabilized when stretched in weft

1 direction and increases when stretched in the warp direction. This behavior can be explained by  
2 considering the arrangements of elastic and non-elastic yarns and shrinkage within the hexagonal  
3 unit cell along warp and weft direction as shown in Figure 4. To make the understanding easier,  
4 the yarn lengths only within the hexagonal unit cell are shown in Figure 4, in which elastic and  
5 non-elastic yarns are presented by the red and black lines, respectively. It can be seen that because  
6 of more elastic yarns at section C in weft direction, there is higher shrinkage along the weft  
7 direction than that along the warp direction. Therefore, when the fabric is stretched along the weft  
8 direction, because of the higher shrinkage along this direction, smaller initial transposition of  
9 shrinkage is achieved and after this the stretching force is consumed in straightening of yarns under  
10 tension. Moreover, because of higher shrinkage at section C, more length of yarns under tension  
11 is needed to be stretched before increase in the distance between points 5 and 6. Consequently, the  
12 increase in transverse dimension is delayed and occurs at higher strains which results in smaller  
13 auxetic effect. In addition, the increase in transverse dimensions occurs simultaneously with  
14 increase in tensile strain which results in stabilized auxetic effect. On the other hand, when the  
15 fabric is stretched along the warp direction, due to the smaller shrinkage along this direction the  
16 higher transposition of shrinkage is achieved at initial tensile strain, resulting in higher initial auxetic  
17 effect. After initial transposition, the stretching force is consumed in straightening of yarns under  
18 tension during which auxetic effect decreases. However, because of smaller shrinkage the  
19 straightening of yarns under tension is achieved earlier, resulting in higher transposition of  
20 shrinkage and auxetic effect increases.



1  
2  
3  
4  
5  
6

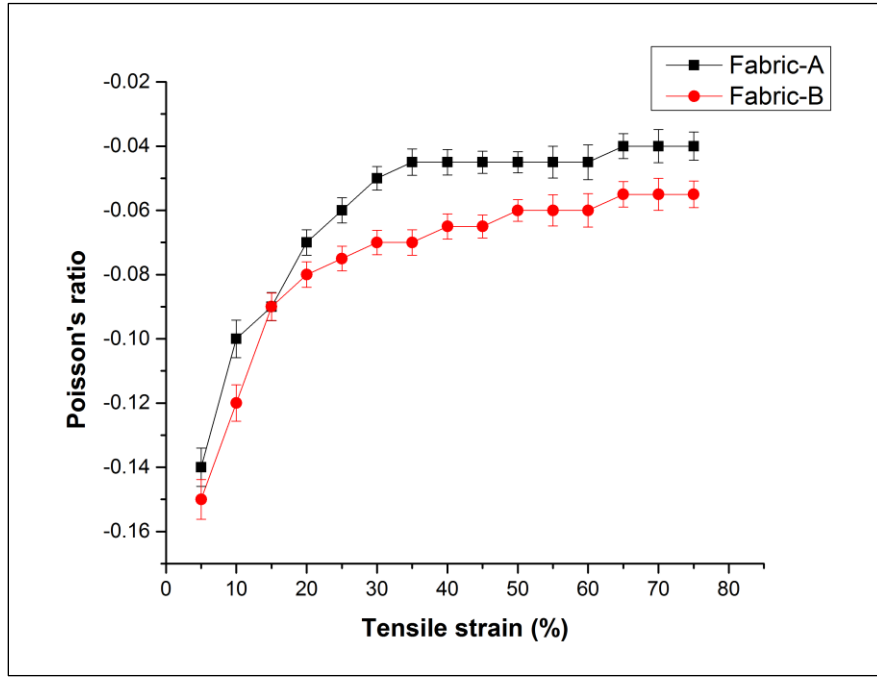
**Figure 4. Explanation of transpose of shrinkage along warp and weft directions: (a) unit cell at free state showing weft yarn arrangement in Fabric-B; (b) unit cell at free state showing weft yarn arrangement in Fabric-A; (c) unit cell at free state showing warp yarn arrangement in fabrics-A & B; (d) unit cell of fabric-B at initial strain stretched along weft direction; (e) unit cell of fabric-A at initial strain stretched along weft direction ; (f) unit cell of fabric-A & B at initial strain stretched along warp direction.**



7

1

Figure 5. Poisson's ratio-tensile strain curves of fabrics when stretched along warp directions.



2

3

Figure 6. Poisson's ratio-tensile strain curves of fabrics when stretched along weft directions.

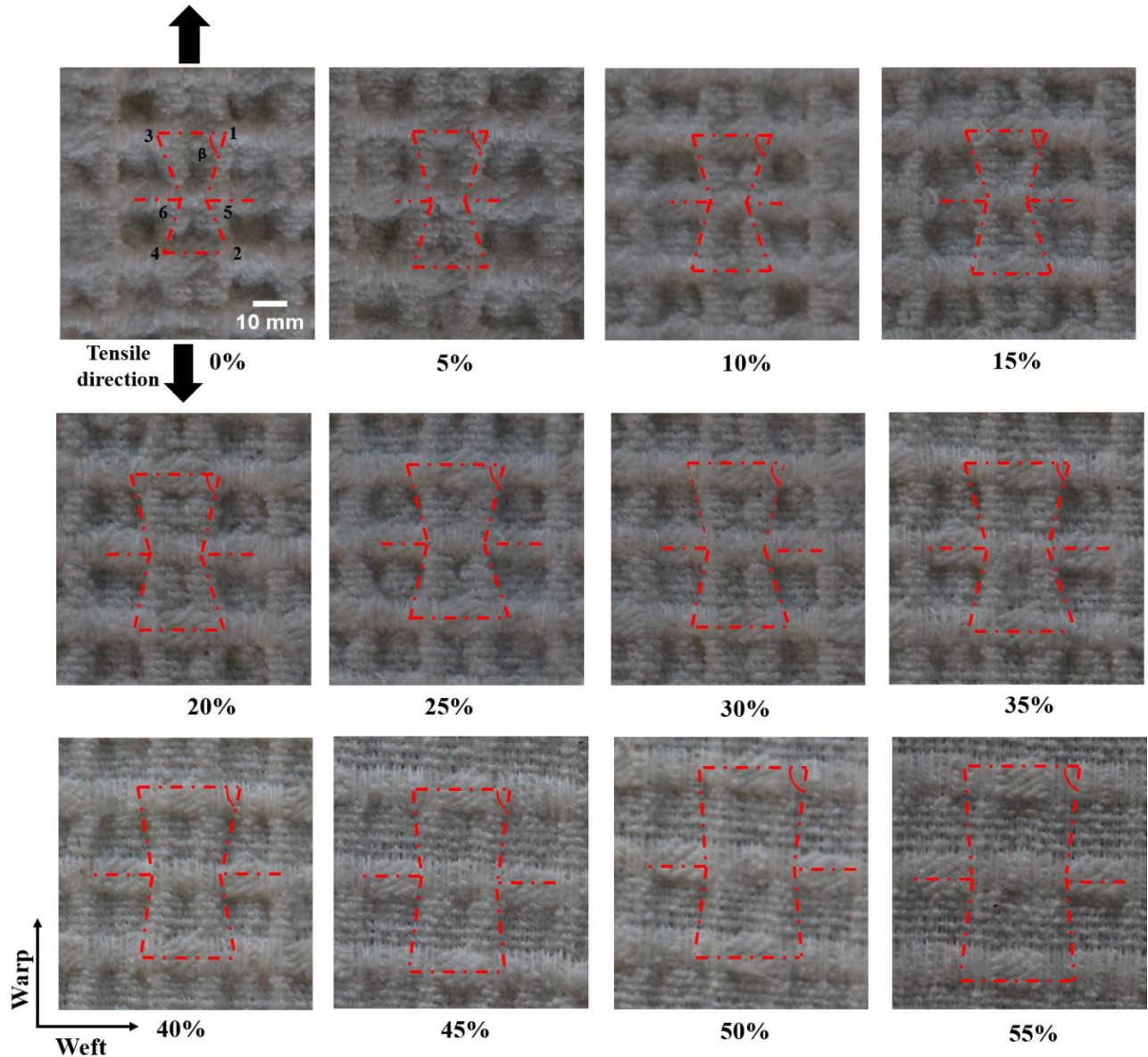
4

### 5 3. Deformation behaviour when stretched in the warp direction

#### 6 3.1 Experimental observations

7 To observe the deformation behaviour of the fabric upon the stretch, the photos were taken at  
8 different tensile strain during the tensile test. Figure 7 shows the five times magnified view of  
9 photos of Fabric-B unit cell at different tensile strain when stretched in the warp direction. The  
10 unit cell of the fabric structure is outlined by dashed lines in all photos. When the fabric is stretched  
11 in the warp direction, the shrinkage at section C transposes and the diagonal segments  $b$  at sections  
12 B tends to move towards the horizontal disposition. Because of this, the angle  $\beta$  formed between  
13 segment  $a$  and  $b$  increases. Therefore, the tensile strain is dependent mainly on the angle  $\beta$ .  
14 Furthermore, the horizontal disposition of diagonal segments makes the distance between point 5  
15 and 6 to increase from the centre in the transverse directions. This increases the dimensions of  
16 the whole fabric structure in the transversal direction to achieve the auxetic effect of the fabric.  
17 Comparing photos of the fabric when stretched in the warp direction, it can be observed that the  
18 deformation of the fabric is likely to be the deformation of the re-entrant hexagonal unit cell  
19 stretched along the long side of the unit cell as outlined in the photos. Therefore, a re-entrant

- 1 hexagonal geometrical model is proposed to estimate the deformation behaviour of the fabric
- 2 structure when stretched in the warp direction.



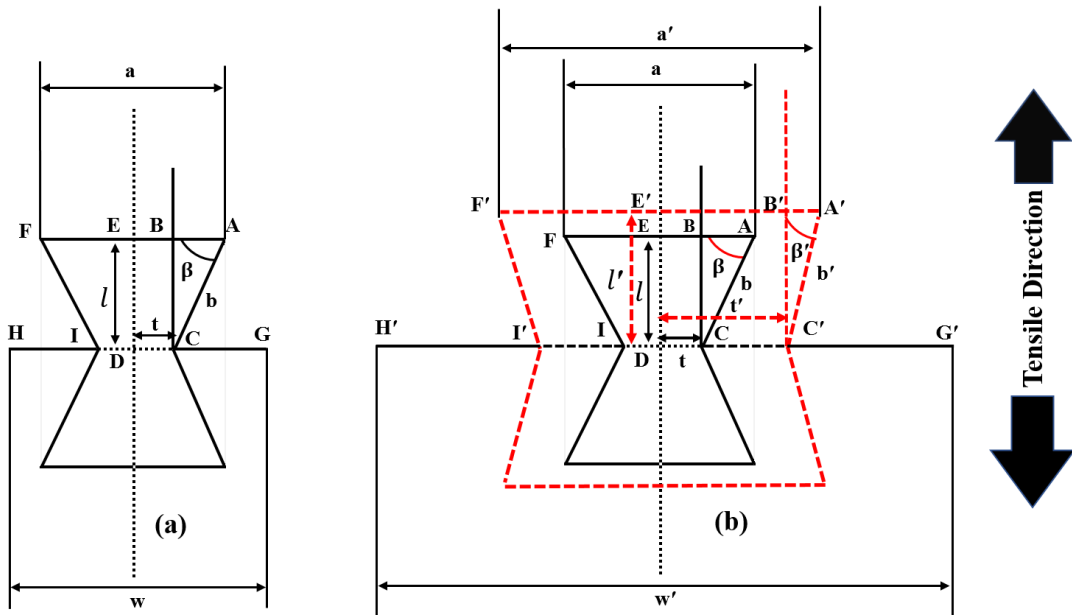
3  
4 **Figure 7. Photos of Fabric-B taken at different tensile strain when stretched in the warp direction**

5 **3.2 Geometrical analysis**

6 To establish the relationship between tensile strain and Poisson's ratio of the developed fabric, the  
 7 geometrical analysis was carried out. A geometrical model, when the fabric is stretched in warp  
 8 direction is proposed as shown in Figure 8. For the simplicity, the following assumptions were  
 9 first made.

- 1 1. The hexagonal unit cells of the fabric structure have the same shape and size and they exhibit
- 2 the same behaviour when the fabric undergoes extension in the warp direction.
- 3 2. The deformation behaviour of the fabric, when the fabric undergoes extension in the warp
- 4 direction can be analyzed by considering the deformation behaviour of the hexagonal unit cell
- 5 under extension along the long side of the unit cell.
- 6 3. All the rib segments are not kept constant due to easy deformation of the fabric structure.

7 Figure 8(a) shows the proposed geometrical model at the free state and Figure 8(b) shows the  
 8 proposed geometrical model at free state (solid lines) as well as a state under extension (dashed  
 9 lines).



10

11 **Figure 8. Geometrical model: (a) the REH geometry unit cell at free state; (b) deformation of the unit cell under extension**  
 12 **in the warp direction.**

13 Considering the geometry of the unit cell before the extension, according to Figure 8(a),  $ABC$  is a  
 14 right-angled triangle before the extension and it changes to  $A'B'C'$  after extension as shown in the  
 15 Figure 8(b). Further, for easy analysis it is supposed that  $AF = a$ ,  $AE = CG = IH = \frac{a}{2} = AB + BE$ ,  
 16  $AC = b$  and  $CD = DI = BE = t$ . Therefore, by applying the geometrical analysis, the following  
 17 relationships can be made between the geometrical parameters at the free state:

1 
$$l = b \sin \beta \quad (4)$$

2 
$$t = \frac{a}{2} - b \cos \beta \quad (5)$$

3 
$$w = a + 2t \quad (6)$$

4 Similarly, considering the geometry of the unit cell after extension, the following relationships can  
5 be made between the geometrical parameters:

6 
$$l' = b' \sin \beta' \quad (7)$$

7 
$$t' = \frac{a'}{2} - b' \cos \beta' \quad (8)$$

8 
$$w' = a' + 2t' \quad (9)$$

9 It can be observed that upon extension in the tensile direction,  $l$  changes to  $l'$  along the tensile  
10 direction and the tensile strain  $\varepsilon_a$  can be obtained as following:

11 
$$\varepsilon_a = \frac{l' - l}{l}$$

12 Substituting  $l$  and  $l'$  with equation (4) and (7) in the above equation gives equation (10):

13 
$$\varepsilon_a = \frac{b' \sin \beta'}{b \sin \beta} - 1 \quad (10)$$

14 From equation (10), the relationship of  $\beta'$  and  $\varepsilon_a$  can be derived as equation (11):

15 
$$\sin \beta' = \frac{(\varepsilon_a + 1)b \sin \beta}{b'} \quad (11)$$

16 From the relationship of  $\sin^2 \beta' + \cos^2 \beta' = 1$ , it can be derived as  $\cos^2 \beta' = \sqrt{1 - \sin^2 \beta'}$  and  
17 substituting  $\sin \beta'$  with equation (11) gives equation (12):

18 
$$\cos \beta' = \sqrt{1 - \left(\frac{(\varepsilon_a + 1)b \sin \beta}{b'}\right)^2} \quad (12)$$

1 Upon extension due to horizontal disposition of  $C$  to  $C'$  in the transverse direction,  $t$  changes to  
 2  $t'$ . As a result, the transverse dimensions of the whole structure increase and  $w$  changes to  $w'$ .  
 3 Therefore, the transverse strain  $\varepsilon_t$  can be obtained as follows.

$$4 \quad \varepsilon_t = \frac{w - w'}{w}$$

5 Substituting  $w$  and  $w'$  with equation (6) and (9) in the above equation gives equation (13):

$$6 \quad \varepsilon_t = \frac{(a' + 2t') - (a + 2t)}{a + 2t} \quad (13)$$

7 Substituting  $t$  and  $t'$  with equation (5) and (8) into equation (13) gives equation (14):

$$8 \quad \varepsilon_t = \frac{a' - b' \cos \beta'}{a - b \cos \beta} - 1 \quad (14)$$

9 Substituting  $\cos \beta'$  with equation (12) into equation (14) gives equation (15) to calculate transverse  
 10 strain:

$$11 \quad \varepsilon_t = \frac{a' - b' \sqrt{1 - \left(\frac{(\varepsilon_a + 1)b \sin \beta}{b'}\right)^2}}{a - b \cos \beta} - 1 \quad (15)$$

12 Substituting equation (15) into equation (3) gives equation (16) which can be used to calculate the  
 13 PR of the fabric, when stretched in the warp direction:

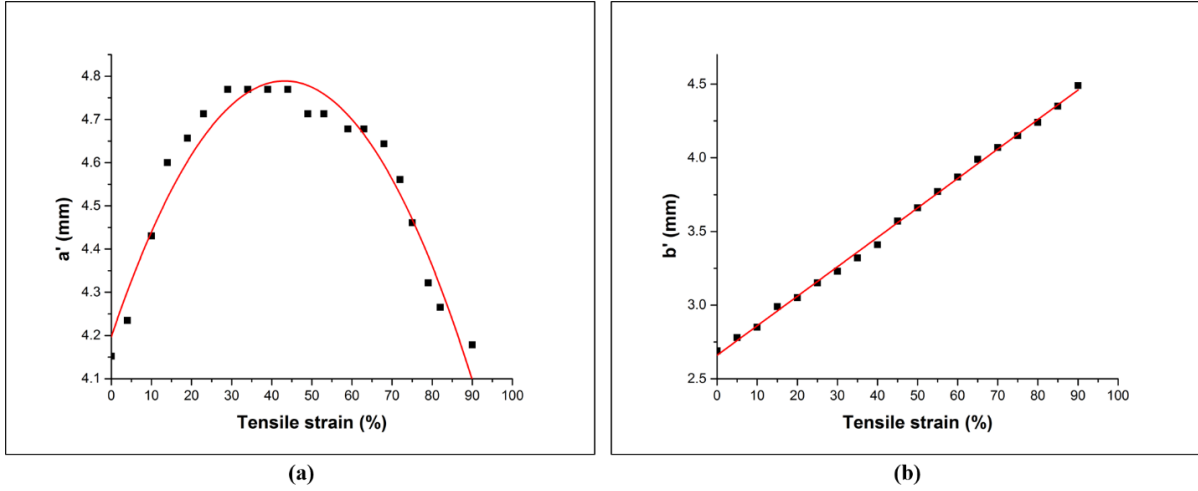
$$14 \quad \nu = \frac{a' - b' \sqrt{1 - \left(\frac{(\varepsilon_a + 1)b \sin \beta}{b'}\right)^2}}{(a - b \cos \beta)\varepsilon_a} - \frac{1}{\varepsilon_a} \quad (16)$$

15 Where  $a, b$  and  $\beta$  are the initial known parameters of the unit cell and  $a', b'$  are the changed  
 16 parameters upon extension. Due to the complicated changes in the fabric structure, it is very  
 17 difficult to determine the exact change of  $a', b'$ . However, from the photos of the fabric unit cell  
 18 taken at different strains, the variation trends of  $a'$  and  $b'$  can be easily determined. The variation  
 19 trends of  $a'$  and  $b'$  as a function of tensile strain are shown in Figure 9. It can be observed that the  
 20 change in  $a'$  has a **parabolic** trend while the change in  $b'$  has a linear trend. Based on these trends,  
 21 the following assumptions about  $a'$  and  $b'$  were established:

1  
2  
3  
4

$$a' = j_1 \varepsilon_a^2 + j_2 \varepsilon_a + j_3 \quad (17)$$

$$b' = b(k\varepsilon_a + 1) \quad (18)$$



5  
6

Figure 9. Variation trend when stretched in the warp direction: (a) trend of  $a'$  ; (b) trend of  $b'$  .

7 Where  $\varepsilon_a$  is the tensile strain of the fabric, when stretched in the warp direction and  $j_1, j_2, j_3$ , and  
 8  $k$  are the constants and can be determined according to the experimental results. Substituting  
 9 equation (17) and (18) into equation (16), then PR of fabric when stretched in the warp direction  
 10 can be derived as the following equation (19):

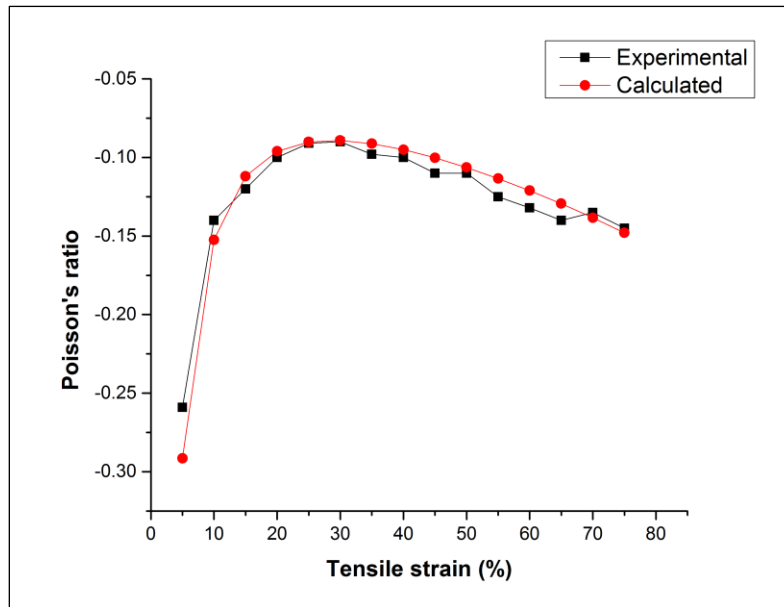
$$v = \frac{(j_1 \varepsilon_a^2 + j_2 \varepsilon_a + j_3) - (b(k\varepsilon_a + 1)) \sqrt{1 - \left(\frac{(\varepsilon_a + 1)b \sin \beta}{b(k\varepsilon_a + 1)}\right)^2}}{(a - b \cos \beta) \varepsilon_a} - \frac{1}{\varepsilon_a} \quad (19)$$

12 From equation (19), it can be found that there are four constants  $j_1, j_2, j_3$ , and  $k$  which are required  
 13 to be determined. The experimental relationship of PR and tensile strain of Fabric-B when  
 14 stretched in the warp direction is used to determine these constants. Therefore, fitting equation  
 15 (19) with the experimental results of Fabric-B gives  $j_1 = -0.0003, j_2 = 0.0274, j_3 = 4.19$  and  
 16  $k = 0.7155$ . Substituting the above values into equation (19) gives a semi-empirical equation (20)

1 which can be used to theoretically calculate the PR of the fabric when the tensile strain is given  
 2 and stretched in the warp direction:

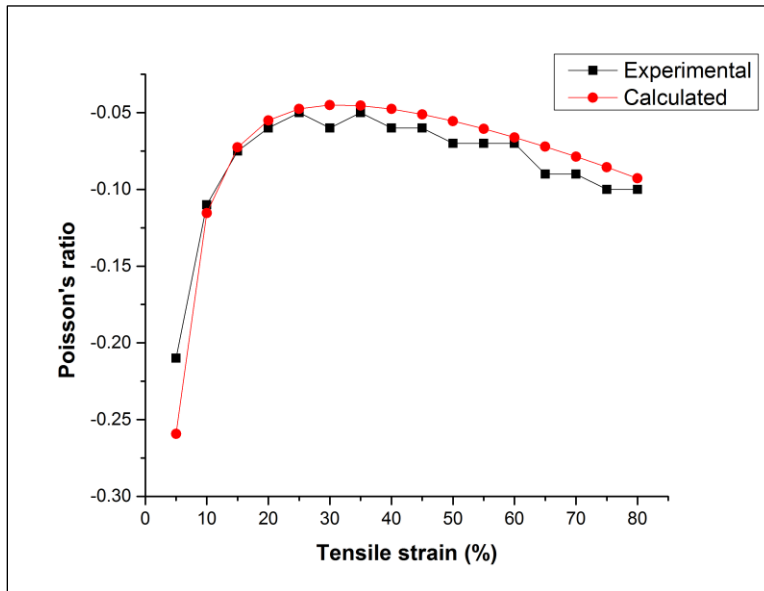
$$3 \quad \nu = \frac{(-0.0003\varepsilon_a^2 + 0.0274\varepsilon_a + 4.19) - (b(0.7155\varepsilon_a + 1))\sqrt{1 - \left(\frac{(\varepsilon_a + 1)b \sin \beta}{b(0.7155\varepsilon_a + 1)}\right)^2}}{(a - b \cos \beta)\varepsilon_a} - \frac{1}{\varepsilon_a} \quad (20)$$

4 Both the calculated and experimental curves of PR vs. tensile strain when the fabric is stretched in  
 5 warp direction are shown in Figure 10. It can be seen that the calculated curve fits well with  
 6 experimental results. To verify equation (20), the testing results of Fabric-A having different value  
 7 of  $\beta$  when stretched in warp direction are compared with the calculated curve which is obtained  
 8 by using equation (20) as shown in Figure 11. It can be seen that the calculated curve fit well with  
 9 the experimental results. Therefore, equation (20) is verified and can be used to predict the PR  
 10 when stretched in warp direction of bi-stretch auxetic woven fabric made of the same type of  
 11 materials and geometry but with different geometrical parameters.



12  
 13 **Figure 10.** Comparison between theoretically calculated curves and experimental results of Fabric-B when stretched in  
 14 **warp direction.**

15  
 16



1  
2 **Figure 11.** Comparison between theoretically calculated curves and experimental results of Fabric-A when stretched in  
3 **warp direction.**

#### 4 **4. Deformation behaviour when stretched in the weft direction**

##### 5 **4.1 Experimental observations when stretched in the weft direction**

6 Figure 12 shows the five times magnified photos of Fabric-B at different tensile strain when  
7 stretched in the weft direction. The unit cell of the fabric structure is outlined in all photos. When  
8 the fabric is stretched in the weft direction, the tensile yarns tend to get straight making the  
9 shrinkage at sections A (segments 1-3, 2-4 or  $a$ ) and at section C to transpose. Because of the  
10 transpose of shrinkage, the diagonal segments  $b$  at section B move towards the horizontal  
11 disposition and translate to the straight form. This horizontal disposition of diagonal segments  
12 makes the distance of point 5 and 6 from the centre to increase in the tensile direction. Therefore,  
13 the tensile strain is mainly dependent on the change in the distance of point 5 and 6 from the centre.  
14 Furthermore, because of increase in the distance of point 5 and 6 from the centre, the angle  $\beta$   
15 formed between segment  $a$  and  $b$  increases which increase the transverse dimensions to achieve  
16 the auxetic effect. Comparing photos of the fabric when stretched in the weft direction, it can be  
17 observed that the deformation of the fabric is likely to be the deformation of the re-entrant  
18 hexagonal unit cell stretched along the short side of the unit cell as outlined in the photos.  
19 Therefore, a re-entrant hexagonal geometrical model is proposed to estimate the deformation  
20 behaviour of the fabric structure when stretched in the weft direction.

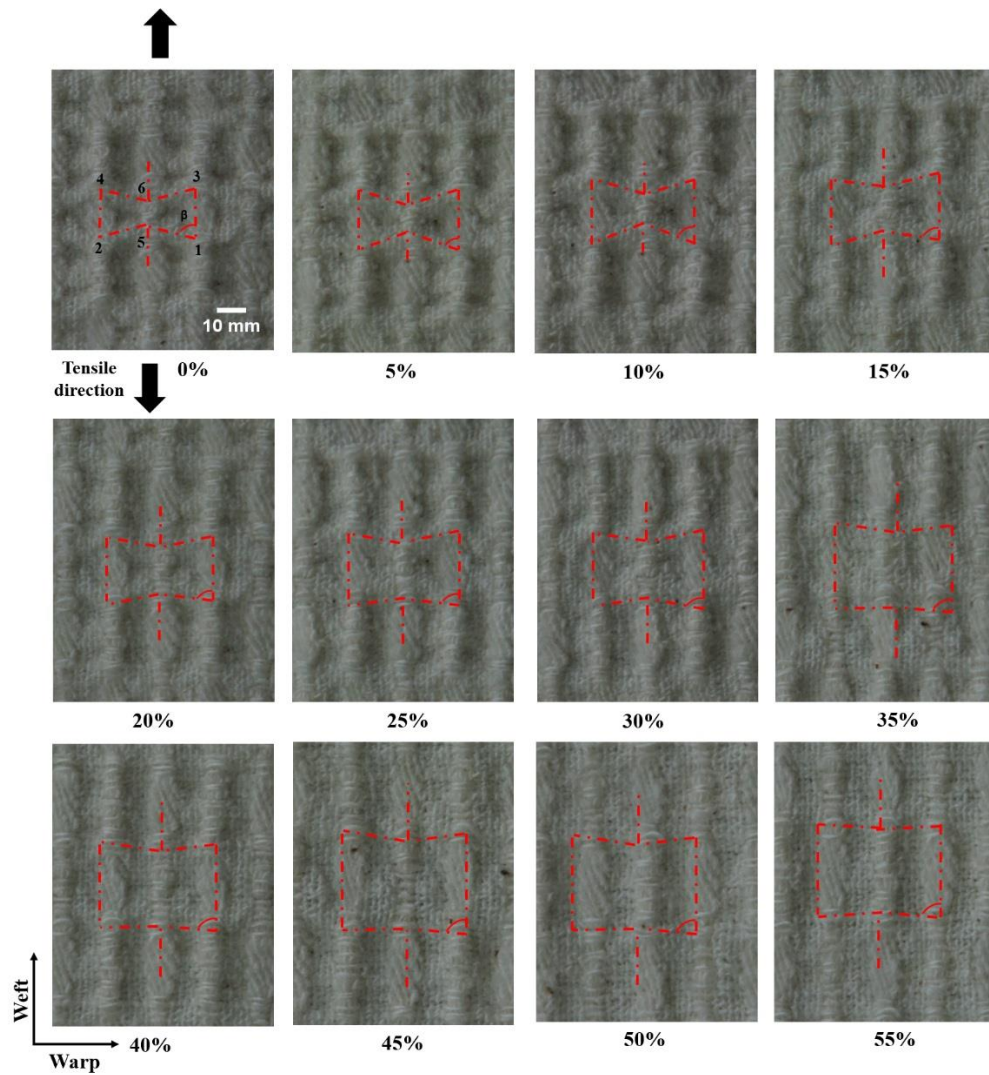


Figure 12. Photos of Fabric-B taken at different tensile strain when the fabric is stretched in the weft direction

#### 4.2 Geometrical analysis when stretched in the weft direction

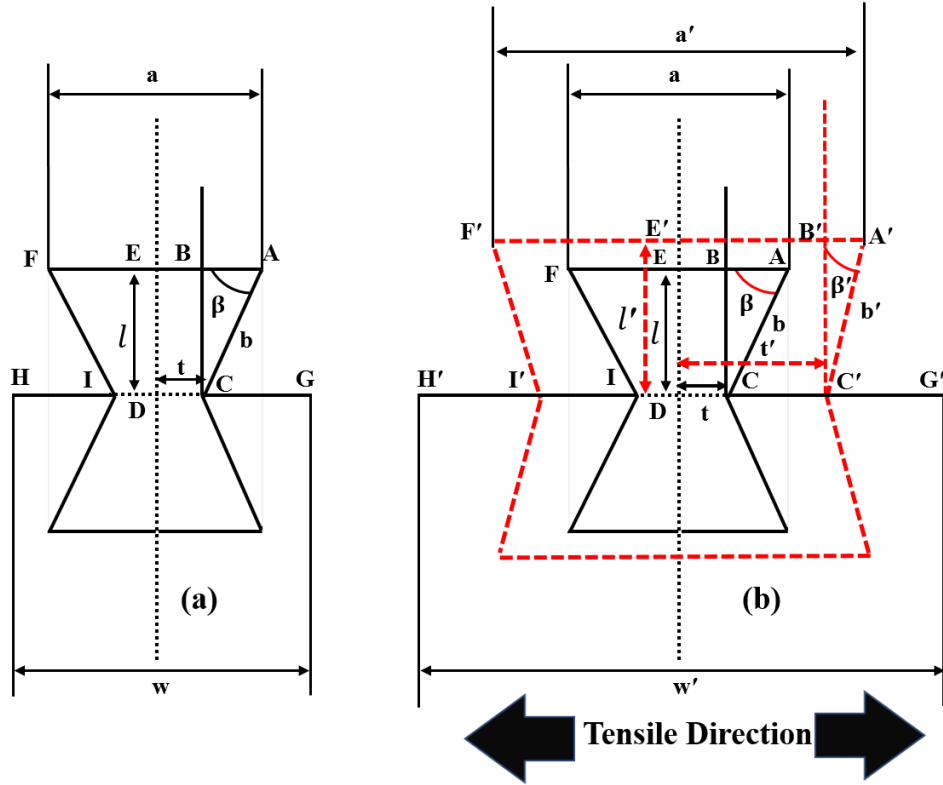
Figure 13 shows a geometrical model when the fabric is stretched in the weft direction. To make the analysis simple, the following assumptions are first made.

1. The hexagonal unit cells of the fabric structure have the same shape and size and they exhibit the same behaviour when the fabric undergoes extension in the weft direction.

2. The deformation behaviour of the fabric can be analyzed by considering the deformation behaviour of the hexagonal unit cell under extension along the short side of the unit cell.

3. All the rib segments are not kept constant due to easy deformation of fabric.

1 Figure 13(a) shows the proposed geometrical model at the free state and Figure 13(b) shows the  
 2 proposed geometrical model at free state (solid lines) as well as a state under extension along the  
 3 short side of the unit cell (dashed lines). Considering the geometry of the unit cell before the  
 4 extension, according to Figure 13(a)  $ABC$  is a right-angled triangle before extension which  
 5 becomes  $A'B'C'$  after extension as shown in Figure 13(b).



6  
 7 **Figure 13. Geometrical model: (a) the REH geometry unit cell at the free state; (b) deformation of the unit cell under**  
 8 **extension in the weft direction.**

9 It can be observed that upon extension in the weft direction,  $w$  increases and changes to  $w'$  and the  
 10 tensile strain  $\varepsilon_a$  can be obtained as follows.

11 
$$\varepsilon_a = \frac{w' - w}{w}$$

12 Substituting  $w$  and  $w'$  with equation (6) and (9) in above equation gives:

13 
$$\varepsilon_a = \frac{(a' + 2t') - (a + 2t)}{a + 2t}$$

14 Substituting  $t$  and  $t'$  with equation (5) and (8) in above equation gives equation (21) for tensile  
 15 strain when stretched in weft direction:

1 
$$\varepsilon_a = \frac{a' - b' \cos \beta'}{a - b \cos \beta} - 1 \quad (21)$$

2 From equation (21) the relationship of  $\beta'$  and  $\varepsilon_a$  can be derived as follows.

3 
$$\cos \beta' = \frac{a' - (\varepsilon_a + 1)(a - b \cos \beta)}{b'} \quad (22)$$

4 From the relationship of  $\sin^2 \beta' + \cos^2 \beta' = 1$ , it can be derived as  $\sin \beta' = \sqrt{1 - \cos^2 \beta'}$  and  
 5 substituting  $\cos \beta'$  with equation (22) gives equation (23).

6 
$$\sin \beta' = \sqrt{1 - \left( \frac{a' - (\varepsilon_a + 1)(a - b \cos \beta)}{b'} \right)^2} \quad (23)$$

7 It can also be observed that upon extension in the weft direction, due to the horizontal disposition  
 8 of  $C$  to  $C'$  and  $I$  to  $I'$  in the tensile direction,  $l$  is increased and changed to  $l'$ . Thus, the transverse  
 9 dimension of the whole fabric structure increases and the transverse strain  $\varepsilon_t$  can be obtained as  
 10 following:

11 
$$\varepsilon_t = \frac{l' - l}{l}$$

12 Substituting  $l$  and  $l'$  with equation (4) and (7) in above equation gives equation (24):

13 
$$\varepsilon_t = \frac{b' \sin \beta'}{b \sin \beta} - 1 \quad (24)$$

14 Substituting  $\sin \beta'$  with equation (23) into equation (24) gives equation (25) to calculate the  
 15 transverse strain when stretched in weft direction:

16 
$$\varepsilon_t = \frac{b' \sqrt{1 - \left( \frac{a' - (\varepsilon_a + 1)(a - b \cos \beta)}{b'} \right)^2}}{b \sin \beta} - 1 \quad (25)$$

17 Finally, the PR  $\nu$  when stretched in the weft direction can be calculated by substituting equation  
 18 (25) into equation (3):

1

$$\nu = \frac{b' \sqrt{1 - \left( \frac{a' - (\varepsilon_a + 1)(a - b \cos \beta)}{b'} \right)^2}}{(b \sin \beta) \varepsilon_a} - \frac{1}{\varepsilon_a} \quad (26)$$

2

3

4

5

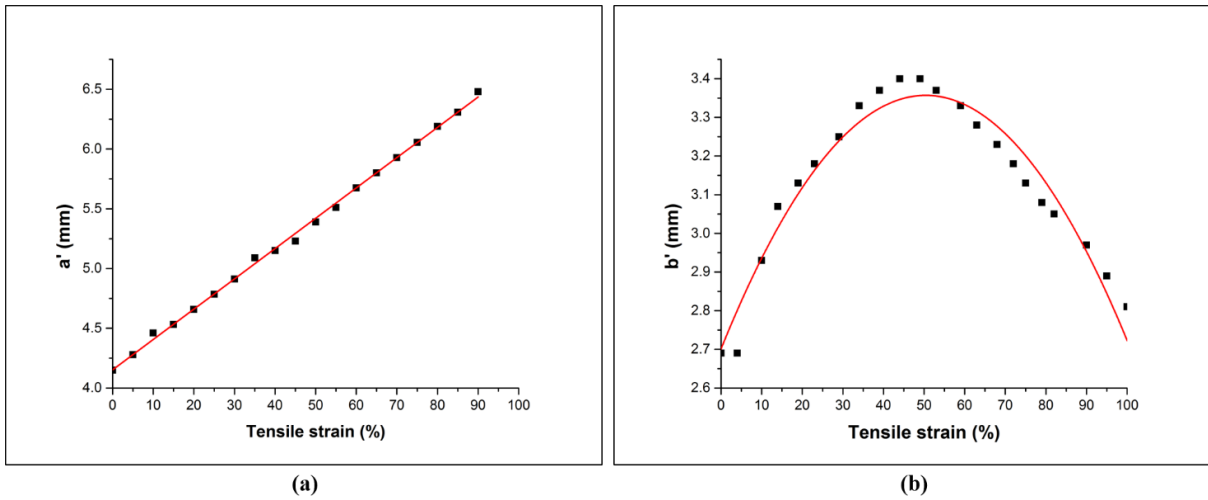
6

7

8

9

Where  $a, b$  and  $\beta$  are the initial known lengths of the rib segments and angle of the unit cell and  $a'$  and  $b'$  are the changed lengths upon extension. Due to the complicated changes in the fabric structure, it is very difficult to determine the exact change  $a$  and  $b$ . However, the change trends can be determined by the fabric photos. Therefore, to calculate the values of  $a'$  and  $b'$ , the photos of the fabric unit cell at different tensile strains when stretched in the weft direction were taken and the changes were measured. It was observed that the change in  $a'$  had a linear trend while the change in  $b'$  had a parabolic trend as shown in Figure 14. Based on these change trends the following assumptions about  $a'$  and  $b'$  were established.



10

11

Figure 14. Variation trends when stretched in the weft direction: (a) trend of  $a'$ ; (b) trend of  $b'$ .

12

$$a' = a(m\varepsilon_a + 1) \quad (27)$$

13

$$b' = n_1 \varepsilon_a^2 + n_2 \varepsilon_a + n_3 \quad (28)$$

14

15

16

17

Where  $\varepsilon_a$  is the tensile strain of the fabric, when stretched in the weft direction and  $m, n_1, n_2$  and  $n_3$  are the constants and can be determined according to the experimental results. Substituting equations (27) and (28) into equation (26), the relationship to calculate the PR  $\nu$  when stretched in the weft direction can be derived as the following equation (29):

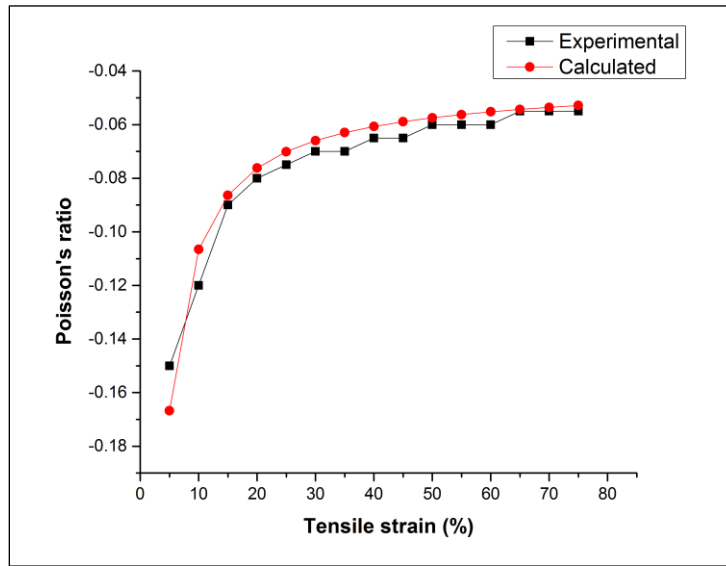
$$1 \quad \nu = \frac{(n_1 \varepsilon_a^2 + n_2 \varepsilon_a + n_3) \sqrt{1 - \left( \frac{a(m \varepsilon_a + 1) - (\varepsilon_a + 1)(a - b \cos \beta)}{n_1 \varepsilon_a^2 + n_2 \varepsilon_a + n_3} \right)^2}}{(b \sin \beta) \varepsilon_a} - \frac{1}{\varepsilon_a} \quad (29)$$

2 In equation (29), it can be found that there are four constants  $m, n_1, n_2$  and  $n_3$  which are required  
3 to be determined. The experimental relationship of PR and tensile strain of Fabric-B when  
4 stretched in the weft direction is used to determine these constants. Therefore, fitting equation (29)  
5 with the experimental results gives  $m = 0.619, n_1 = -0.0003, n_2 = 0.0258$  and  $n_3 = 2.7012$  .  
6 Substituting the above values into equation (29) gives a semi-empirical equation (30) which can  
7 be used for theoretically calculating the PR of the fabric for a given tensile strain when the fabric  
8 is stretched in the weft direction:

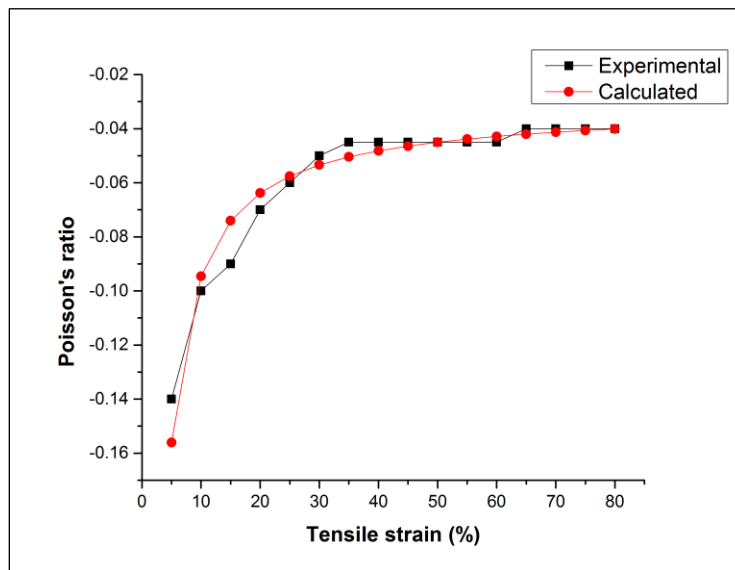
$$9 \quad \nu = \frac{(-0.0003 \varepsilon_a^2 + 0.0258 \varepsilon_a + 2.7012) \sqrt{1 - \left( \frac{a(0.619 \varepsilon_a + 1) - (\varepsilon_a + 1)(a - b \cos \beta)}{(-0.0003 \varepsilon_a^2 + 0.0258 \varepsilon_a + 2.7012)} \right)^2}}{(b \sin \beta) \varepsilon_a} - \frac{1}{\varepsilon_a} \quad (30)$$

10 Both the calculated curve and experimental values of PR are shown in Figure 15. It can be observed  
11 that the calculated curve fits well with experimental results. To verify equation (30), the testing  
12 results of Fabric-A having different value of  $\beta$  when stretched in weft direction are compared with  
13 the calculated curve which is obtained by using equation (30) as shown in Figure 16. The  
14 calculated curve fit well with the experimental results. Therefore, equation (30) is verified and can  
15 be used to predict the PR of bi-stretch auxetic woven fabric made of the same type of materials  
16 and geometry but with different values of geometrical parameters when stretched in weft direction.

17  
18  
19  
20



1  
2 **Figure 15.** Comparison between theoretically calculated curves and experimental results of Fabric-B when stretched in  
3 weft direction.

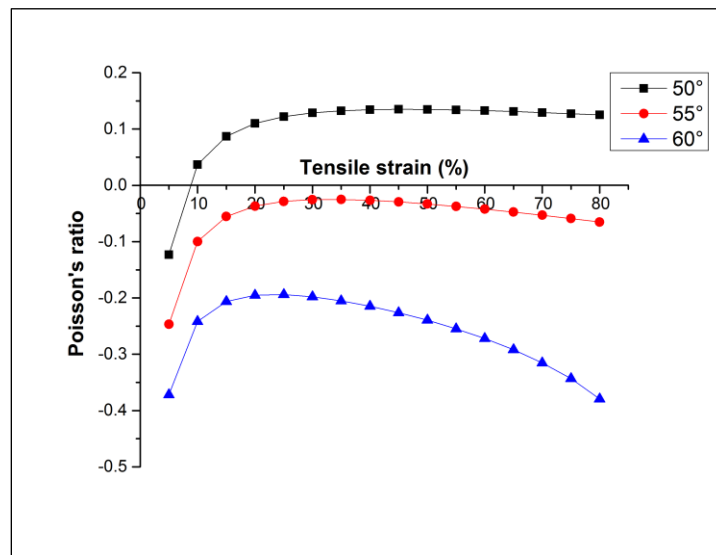


4  
5 **Figure 16.** Comparison between theoretically calculated curves and experimental results of Fabric-A when stretched in  
6 weft direction.

7 **5. Prediction of auxetic behavior**

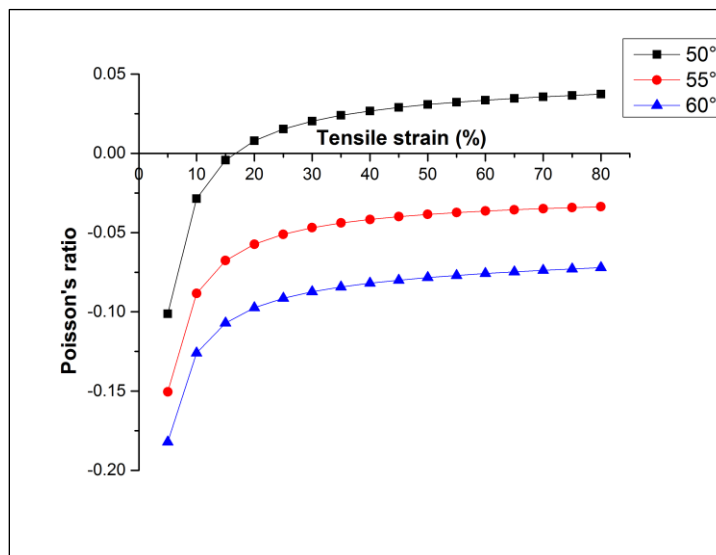
8 From equation (20) and equation (30), it can be seen that the PR of the fabric when stretched in  
9 warp or weft direction depends on  $\beta$ . To study the effect of  $\beta$  on the PR of fabric, the PR of the  
10 fabric is calculated for different values of  $\beta$  and PR curves are plotted as a function of the tensile  
11 strain for different values of  $\beta$  using equation (20) when stretched in warp direction and equation  
12 (30) when stretched in weft direction. The prediction curves for both stretching directions are

1 presented in Figure 17 and Figure 18, respectively. It is evident from the prediction curves that  
 2 when the fabrics is stretched in either direction, the auxetic effect rapidly increases with increase  
 3 of  $\beta$ . This behavior can be explained by the fact that the larger the value of  $\beta$ , the less will be the  
 4 shrinkage at section C. Thus, the straightening of tensile yarns will achieve earlier resulting in  
 5 higher transpose of shrinkage even at smaller strains which will increase the auxetic effect.  
 6 Therefore, to design a bi-stretch auxetic woven fabric based on REH geometry a higher value of  
 7  $\beta$  is more suitable.



8  
9

Figure 17. Effect of  $\beta$  on the Poisson's ratio of fabric when stretched in warp direction.



10  
11

Figure 18. Effect of  $\beta$  on the Poisson's ratio of fabric when stretched in weft direction.



- 1 [5] H. Hu and A. Zulifqar, "Auxetic textile materials-A review," *J Textile Eng Fashion Technol*, vol. 1, p.  
2 00002, 2016.
- 3 [6] T. C. Lim, "Semi - auxetic yarns," *physica status solidi (b)*, vol. 251, pp. 273-280, 2014.
- 4 [7] Z. Wang and H. Hu, "Tensile and forming properties of auxetic warp-knitted spacer fabrics," *Textile  
5 Research Journal*, vol. 87, pp. 1925-1937, 2017.
- 6 [8] A. Toronjo, "Articles of apparel including auxetic materials," ed: US Patent 9,629,397, 2017.
- 7 [9] V. Monika and V. Petra, "Auxetic woven fabrics—pores' parameters observation auxetic woven  
8 fabrics—pores' parameters observation," *Journal of Donghua University (English)*. vol. 5, pp. 71-  
9 75, 2013.
- 10 [10] J. R. Wright, M. K. Burns, E. James, M. R. Sloan, and K. E. Evans, "On the design and characterisation  
11 of low-stiffness auxetic yarns and fabrics," *Textile Research Journal*, vol. 82, pp. 645-654, 2012.
- 12 [11] N. Grimmelsmann, H. Meissner, and A. Ehrmann, "3D printed auxetic forms on knitted fabrics for  
13 adjustable permeability and mechanical properties," in *IOP Conference Series: Materials Science  
14 and Engineering*, 2016, p. 012011.
- 15 [12] M. Sloan, J. Wright, and K. Evans, "The helical auxetic yarn—a novel structure for composites and  
16 textiles; geometry, manufacture and mechanical properties," *Mechanics of Materials*, vol. 43, pp.  
17 476-486, 2011.
- 18 [13] W. S. Ng and H. Hu, "Woven Fabrics Made of Auxetic Plied Yarns," *Polymers*, vol. 10, p. 226, 2018.
- 19 [14] P. Ma, Y. Chang, and G. Jiang, "Design and fabrication of auxetic warp-knitted structures with a  
20 rotational hexagonal loop," *Textile Research Journal*, vol. 86, pp. 2151-2157, 2016.
- 21 [15] K. Alderson, A. Alderson, S. Anand, V. Simkins, S. Nazare, and N. Ravirala, "Auxetic warp knit textile  
22 structures," *physica status solidi (b)*, vol. 249, pp. 1322-1329, 2012.
- 23 [16] S. C. Ugbolue, Y. K. Kim, S. B. Warner, Q. Fan, C.-I. Yang, and O. Kyzymchuk, "Auxetic fabric  
24 structures and related fabrication methods," ed: US Patent 8,772,187, 2014.
- 25 [17] S. C. Ugbolue, Y. K. Kim, S. B. Warner, Q. Fan, C.-L. Yang, O. Kyzymchuk, *et al.*, "The formation and  
26 performance of auxetic textiles. Part I: theoretical and technical considerations," *the Journal of  
27 the Textile Institute*, vol. 101, pp. 660-667, 2010.
- 28 [18] S. C. Ugbolue, Y. K. Kim, S. B. Warner, Q. Fan, C. L. Yang, O. Kyzymchuk, *et al.*, "The formation and  
29 performance of auxetic textiles. Part II: geometry and structural properties," *The Journal of The  
30 Textile Institute*, vol. 102, pp. 424-433, 2011.
- 31 [19] Z. Wang and H. Hu, "3D auxetic warp - knitted spacer fabrics," *physica status solidi (b)*, vol. 251,  
32 pp. 281-288, 2014.
- 33 [20] Y. Liu, H. Hu, J. K. Lam, and S. Liu, "Negative Poisson's ratio weft-knitted fabrics," *Textile Research  
34 Journal*, vol. 80, pp. 856-863, 2010.
- 35 [21] H. Hu, Z. Wang, and S. Liu, "Development of auxetic fabrics using flat knitting technology," *Textile  
36 Research Journal*, vol. 81, pp. 1493-1502, 2011.
- 37 [22] F. Steffens, S. Rana, and R. Figueiro, "Development of novel auxetic textile structures using high  
38 performance fibres," *Materials & Design*, vol. 106, pp. 81-89, 2016.
- 39 [23] M. Glazzard and P. Breedon, "Weft - knitted auxetic textile design," *physica status solidi (b)*, vol.  
40 251, pp. 267-272, 2014.
- 41 [24] A. Boakye, Y. Chang, K. R. Rafiu, and P. Ma, "Design and manufacture of knitted tubular fabric with  
42 auxetic effect," *The Journal of The Textile Institute*, vol. 109, pp. 596-602, 2018.
- 43 [25] H. Cao, A. Zulifqar, T. Hua, and H. Hu, "Bi-stretch auxetic woven fabrics based on foldable  
44 geometry," *Textile Research Journal*, vol. 0, p. 0040517518798646.
- 45 [26] A. Zulifqar and H. Hu, "Development of Bi - Stretch Auxetic Woven Fabrics Based on Re - Entrant  
46 Hexagonal Geometry," *physica status solidi (b)*, p.1800172, 2018.
- 47 [27] T. Ferrero-Regis, "Twenty-first century dandyism: fancy Lycra® on two wheels," *Annals of Leisure  
48 Research*, vol. 21, pp. 95-112, 2018.

- 1 [28] R. Atakan, H. A. Tufan, H. Baskan, S. Eryuruk, N. Akalin, H. Kose, *et al.*, "Design of an Electronic  
2 Chest-Band," in *IOP Conference Series: Materials Science and Engineering*, 2017, p. 072002.
- 3 [29] A. Marmarali, G. Ertekin, N. Oğlakcioğlu, M. Kertmen, and İ. S. Aydın, "New knitted fabric concepts  
4 for denim products," in *IOP Conference Series: Materials Science and Engineering*, 2017, p.  
5 092002.
- 6 [30] T.-C. Lim, *Auxetic Materials and Structures*. Singapore: Springer, 2015.

7

8